Z. Phys. C – Particles and Fields 49, 401–409 (1991)

Zeitschrift für Physik C Particles and Fields
© Springer-Verlag 1991

A measurement of the π^0, η and η' electromagnetic form factors

CELLO Collaboration

H.-J. Behrend, L. Criegee, J.H. Field[1], G. Franke, H. Jung[2], J. Meyer, O. Podobrin, V. Schröder, G.G. Winter
Deutsches Elektronen-Synchrotron, DESY, W-2000 Hamburg, Federal Republic of Germany

P.J. Bussey, A.J. Campbell, D. Hendry, S.J. Lumsdon, I.O. Skillicorn
University, Glasgow, UK

J. Ahme, V. Blobel, M. Feindt, H. Fenner, J. Harjes, J.H. Köhne[3], J.H. Peters, H. Spitzer, T. Weihrich
II. Institut für Experimentalphysik, Universität Hamburg, W-2000 Hamburg, Federal Republic of Germany

W.-D. Apel, J. Engler, G. Flügge[2], D.C. Fries, J. Fuster[4], K. Gamerdinger[5], P. Grosse-Wiesmann[6], H. Küster[7], H. Müller, K.H. Ranitzsch, H. Schneider
Kernforschungszentrum Karlsruhe und Universität Karlsruhe, W-7500 Karlsruhe, Federal Republic of Germany

W. de Boer[3], G. Buschhorn, G. Grindhammer, B. Gunderson, C. Kiesling, R. Kotthaus, H. Kroha[8], D. Lüers, H. Oberlack, P. Schacht, S. Scholz, W. Wiedenmann[6]
Max Planck-Institut für Physik und Astrophysik, W-8000 München, Federal Republic of Germany

M. Davier, J.F. Grivaz, J. Haissinski, V. Journé, F. Le Diberder[9], J.-J. Veillet
Laboratoire de l'Accélérateur Linéaire, Orsay, France

K. Blohm, R. George, M. Goldberg, O. Hamon, F. Kapusta, L. Poggioli, M. Rivoal
Laboratoire de Physique Nucléaire et des Hautes Energies, Université de Paris, France

G. d'Agostini, F. Ferrarotto, M. Iacovacci, G. Shooshtari, B. Stella
University of Rome and INFN, Rome, Italy

G. Cozzika, Y. Ducros
Centre d'Etudes Nucléaires, Saclay, France

G. Alexander, A. Beck, G. Bella, J. Grunhaus, A. Klatchko[10], A. Levy, C. Milstène
Tel Aviv University, Tel Aviv, Israel

Received 3 October 1990

Abstract. We present measurement of the $\pi^0\gamma^*\gamma$, $\eta\gamma^*\gamma$ and $\eta'\gamma^*\gamma$-transition form factors. The π^0-form factor is for the first time observed in the space-like region. The transition form factor of the η-meson is determined from its decay modes $\pi^+\pi^-\pi^0$, $\pi^+\pi^-\gamma$ and the neutral decay mode $\gamma\gamma$. The decay of the η' is observed in the decay channels $\rho\gamma$, $\eta\pi^+\pi^-$ with $\eta\to\gamma\gamma$ and in the four charged prong final state stemming from $\eta\pi^+\pi^-$ with the η decaying into $\pi^+\pi^-(\pi^0/\gamma)$. All form factors agree well with a simple ρ-pole predicted by the vector meson dominance model and also with the QCD inspired Brodsky-Lepage model.

[1] Now at Université de Genève, Switzerland
[2] Now at RWTH, Aachen, FRG
[3] Now at Univ. Karlsruhe, FRG
[4] Now at Inst. de Física Corpuscular, Universidad de Valencia, Spain
[5] Now at MPI für Physik und Astrophysik, München, FRG
[6] Now at CERN, Geneva, Switzerland
[7] Now at DESY, Hamburg, FRG
[8] Now at Univ. of Rochester, USA
[9] Now at Stanford Linear Accelerator Center, USA
[10] Now at University of California, Riverside, USA

1 Introduction

The reaction $e^+e^-\to\pi^+\pi^-$ is dominated below 1 GeV by the formation of the ρ resonance. From this it follows

that the elastic scattering of an electron off a charged pion should also be dominated by a diagram in which the virtual photon couples to hadronic matter via a ρ. This is the hypothesis of ρ-pole dominance; it can be generalised by the inclusion of further vector meson diagrams to give various forms of the vector meson dominance model for the interaction of real and virtual photons with hadrons.

The presence of vector meson diagrams can be interpreted as an effective mean charge radius at low q^2, the squared mass of the exchanged virtual photon. The Coulomb form factor will be changed to higher values in the time-like region and to lower values in the space-like region. A number of groups have measured the form factor of the charged pion. It can be extracted from measurements of the electromagnetic process $ep \to e\pi^+ n$ [1–3]; a more direct method is to measure the elastic scattering of pions off atomic electrons [4–6]. The latter method is more precise, but is in practice limited to fairly low values of $Q^2 = -q^2$.

From C-symmetry the elastic Coulomb form factor of the π^0 vanishes. However, one can access the electromagnetic vertex behaviour of the neutral pion in the reaction $\pi^0 \to \gamma\gamma^*$. This reaction is described by the amplitude $T_{\mu\nu} = i\varepsilon_{\mu\nu\alpha\beta} \cdot q_1^\alpha \cdot q_2^\beta \cdot F(Q_1^2, Q_2^2)$ in terms of the $\pi^0 - \gamma$-*transition form factor* $F(Q_1^2, Q_2^2)$. If only one of the Q_i^2 deviates substantially from zero the form factor is assumed to factorize into $F(Q_1^2) \cdot F(Q_2^2)$. Usually a pole form is chosen to characterize the Q^2-development of the form factor ($F(Q^2) \propto 1/(1 + Q^2/\Lambda^2)$). The slope b of the form factor at $Q^2 = 0$ is a measure for the density radius of the charged pions and for the size of the interaction region for neutral mesons. Measurements of this form factor in the time-like region ($q^2 > 0$) are obtained by an analysis of the lepton pair spectrum in conversion decays $\pi^0 \to \gamma e^+ e^-$ (for a review see [7]).

In the present experiment we have for the first time measured the form factor of the neutral pion in the space-like region. We have also measured the form factors of the η and η'-mesons in variety of decay channels, some of which (e.g. $\eta \to \gamma\gamma$ and $\eta' \to \pi^+\pi^-\eta$, $\eta \to \pi^+\pi^-(\pi^0/\gamma)$) have not previously been studied for this purpose.

We make use of the two photon process $\gamma\gamma \to P$, (P = pseudoscalar meson), where the two photons are radiated virtually by colliding e^+e^- beams. One of the virtual photons in the reaction is almost real; the other has a larger Q^2 value and is tagged by detecting an e^+ or e^- emerging at a finite angle relative to its original direction.

The paper is organized as follows. First we describe the detector components relevant for the form factor measurements. The selection of events and the analysis method for the π^0 form factor determination are presented in Sect. 3. This is followed by the analysis of the various η-decay modes. In Sect. 5 we present a precise determination of the η' radiative width is used in Sect. 6 for the form factor measurement of this resonance as a normalisation point at $Q^2 = 0$. Pole form fits have been performed on all measured data points. The results of these fits are presented in Sect. 7 and compared with other measurements in the time-like and space-like region. The last Sect. of this paper will summarize the measurements.

2 Apparatus

The data were taken with the CELLO detector at the PETRA storage ring at a centre of mass energy of 35 GeV and correspond to an integrated luminosity of 86 pb^{-1}. A detailed description of the CELLO detector is given elsewhere [8]. Charged tracks are reconstructed in the central detector consisting of nine cylindrical drift chambers and five proportional chambers in a 1.3 T magnetic field provided by a superconducting solenoid, yielding a momentum resolution of $\sigma(p)/p = 0.02 \cdot p$ (p in GeV/c) which can be improved by a vertex constraint. The central detector is surrounded by a fine grained lead-liquid argon calorimeter consisting of 16 barrel and 4 end cap modules. The modules are divided longitudinally into layers, each containing several lead sheets and read-out strips in different directions. The angular resolution of photon showers is 4 mrad. The energy resolution is $\sigma(E)/E = 10\%/\sqrt{E} + 5\%$. In the acceptance gap between the end cap and barrel calorimeter a system of "hole tagger" counters consisting of two scintillator sheets with a lead plate in between gives detection of photons and charged particles above 200 MeV.

The identification and removal of background in the calorimeter, due to noise and charged pion reactions in the coil, is achieved by means of its good spatial resolution in both the longitudinal and the lateral direction. For this analysis the standard reconstruction was extended to achieve a higher acceptance of both low $p_\perp$ charged particles and low energy photons in the liquid argon barrel and end cap calorimeters. The latter is made possible by a detailed knowledge of the noise behaviour of all individual channels over periods of about one week of running. This information was incorporated into the Monte Carlo.

Candidate events for the process $\gamma\gamma \to \pi^0$ were recorded using a trigger which required (1) substantial energy in one or more of the liquid argon barrel modules, and (2) an electromagnetic shower in either the forward detector detector or end cap calorimeter. The energy thresholds were approximately 800 MeV in the barrel (as measured using an FADC), and 2 GeV in the forward detectors and end caps.

Low multiplicity hadronic events were triggered by a fast track-finding processor [9], which basically required two tracks with transverse momentum p_T above 650 MeV/c, or two tracks above 250 MeV/c with an opening angle $\Delta\phi > 45°$ in the plane perpendicular to the beam (135° for part of the experiment). By applying the same algorithm to the hit pattern of Monte Carlo events, the trigger decision was reliably simulated.

For this analysis one of the scattered beam leptons (the "tag") had to be detected in either the end cap calorimeters (100–400 mrad) or in one of the forward calorimeters (40–100 mrad) consisting of lead glass blocks and a set of scintillator rings. In either case a minimum energy of 5 GeV (7 GeV for the π^0 analysis) was subsequently imposed for a tag to be accepted.

3 The π^0 form factor

Events containing two final-state photons were generated in exclusive processes of interest such as $\gamma\gamma \to \pi^0$, $\gamma\gamma \to \eta$ and $\gamma\gamma \to \eta'$, but could also arise from processes containing additional unobserved π^0's. In addition, there exists a possible background from cosmic rays and beam-gas scattering. Consequently, great care was taken with the photon identification in the liquid argon. The reconstruction program identified clusters of neighbouring strips firing in the liquid argon modules, associated these into groups which could correspond to electromagnetic showers, and evaluated the associated shower energy. Full account was taken of variations in the calibration constants, and of the presence of dead channels. Complete information was retained on the DST concerning the amounts of energy deposited in the different layers of the liquid argon. The liquid argon signals were finally classified as

(1) energy associated with a charged track;
(2) well-measured photons;
(3) badly measured photons;
(4) neutral hadron showers;
(5) noise.

Class (1) did not contribute to the π^0 analysis, apart from a small number of wide angle end cap tags. For present purposes, photons were taken to be "badly measured" if their measured energy was less than 100 MeV, or if they were detected within 4 cm of the inner boundaries of any of the liquid argon modules. At the ends of the barrel, an angular cut-off at $|\cos\vartheta| < 0.87$ relative to the beam line was imposed.

A signal was called "neutral hadronic" if its profile did not correspond to that of an electromagnetic shower; the main requirement was that at least 30% of the energy should be deposited in the first four layers of the module. Noise signals were those with a small number of strips firing, or else all firing strips consistent with normal noise fluctuations. The Monte Carlo simulation of the lead liquid argon included experimentally observed levels of noise in the various channels.

After excluding all events with charged tracks (unless associated with an end cap tag), an event was retained as a π^0 candidate if it had precisely two well-measured barrel photons, no noise photons above 100 MeV, no badly measured photons and no "neutral hadron" signals. It was rejected if any signal was found in the hole tagger counters, or any signals above 100 MeV in the end caps which was not associated with a tag. The events were scanned by eye to identify any with signs of an unreconstructed charged track, and a cut was applied to require the $\gamma\gamma$-system to be opposite to the tag in azimuth to within $\pm 20°$. Only small numbers of events were removed by these rejections. The total $\gamma\gamma$-energy in the barrel was required to be at least 700 MeV, and a tag energy of at least 7 GeV was demanded.

The final energy calibration of the barrel modules was carried out by selecting events of the type $e^+e^- \to e^+e^-e^+e^-$ (i.e. $\gamma\gamma \to e^+e^-$), and by matching the energies of the showers in the liquid argon with those of the corresponding charged tracks. A similar calibration was performed for Monte Carlo simulated electron-positron events. After the data and Monte Carlo e^+/e^- tracks had been made to give correct mean shower energies, Monte Carlo photon showers were generated and compared with the simulated e^+/e^- showers. A small correction relative to the e^+/e^- showers was found to be needed, and a similar correction was applied to the photon signals in the data. The end caps were calibrated using Bhabha events.

The shape of the energy threshold of the liquid argon trigger was determined by examining $\gamma\gamma \to e^+e^-$ events in which just one e^+/e^- entered a barrel liquid argon module. These events were triggered by a charged track trigger in addition to the possibility of a liquid argon trigger. The fraction of electrons which generated a liquid argon trigger was evaluated as a function of their energy, and the resulting curve incorporated into the Monte Carlo simulation of the processes. The efficiency of the forward tagger trigger (96%) was evaluated by finding the fraction of those alternatively triggered events with a forward tag signal which fired the forward tag trigger.

Events with tagging electrons (positrons) at angles in the range 40–90 mrad were used in the analysis. The behaviour of the forward tagger was studied by means of tagged events of the types $\gamma\gamma \to e^+e^-$ and $\gamma\gamma \to \mu^+\mu^-$. The energies and momenta of the observed charged tracks gave a prediction of the energy and angle of the tag (assuming that the other final-state beam lepton travelled along the beam line). From this, the signals from

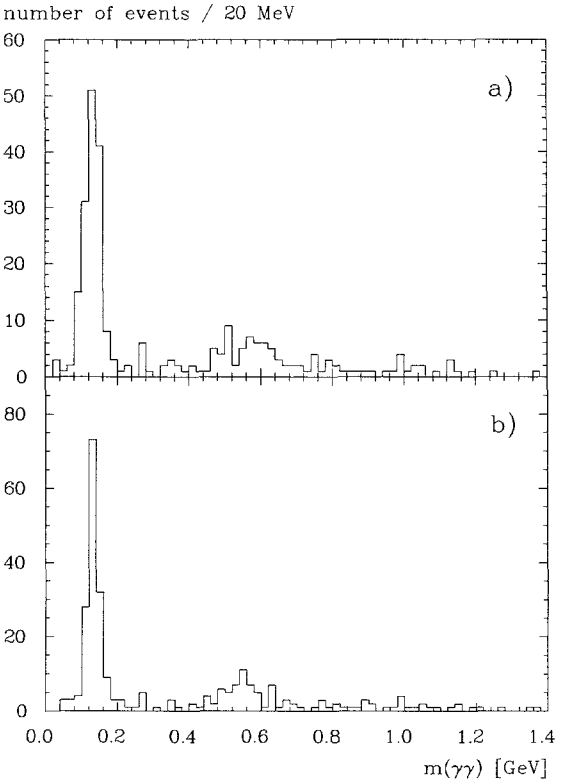

Fig. 1a, b. Effective mass of tagged photon pairs observed in the barrel liquid argon calorimeter **a** before **b** after transverse momentum fit (see text)

the forward taggers could be calibrated. A similar study was performed on Monte Carlo simulated events of the same type. In this way, the Monte Carlo simulation of the forward taggers could be compared with the real data, and appropriate correction factors incorporated in the Monte Carlo analysis. These were angle-dependent and were within $\pm 20\%$ of unity within most of the angle range, rising to a 50% correction at 90 mrad.

The $\gamma\gamma$-mass spectrum of the selected events with a forward tag is shown in Fig. 1a. Clear π^0 and η signals are seen to the appropriate masses. (About 5 η' events might be expected at masses around 1 GeV.) A fit to the photon energies was now applied to constrain the transverse momentum of the $\gamma\gamma$-pair to equal that of the tag. The results are plotted in Fig. 1b, which shows a significant reduction in the width of the peaks. Cuts were applied to Fig. 1b to isolate the π^0 and η signals in the mass ranges 80–180 MeV and 400–700 MeV respectively. Sidebands were defined in the ranges 40–80, 180–300 MeV for the π^0, and 250–400, 700–850 MeV for the η. Background subtractions were applied using these sidebands.

In addition to the backgrounds from photon pairs which did not arise from a π^0 or η, certain classes of events could give $\gamma\gamma$ peaks at the π^0 or η mass. Simulations were performed of the processes $\gamma\gamma \to \eta \to 3\pi^0$, $\gamma\gamma \to \eta' \to \eta\pi^0\pi^0 \to 5\pi^0$, $\gamma\gamma \to \eta' \to \eta\pi^0\pi^0 \to \gamma\gamma\pi^0\pi^0$, $\gamma\gamma \to a_2(1320) \to \pi^+\pi^-\pi^0$, $\gamma\gamma \to a_2(1320) \to \eta\pi^0\pi^0 \to \gamma\gamma\pi^0\pi^0$, and $\gamma\gamma \to f_2(1270) \to \pi^0\pi^0$. In addition, simulations were performed of e^+e^- annihilation into hadrons (including initial state radiation), and the process $\gamma\gamma \to$ hadrons (tagged and untagged) using standard cross sections, and multiply radiative Bhabha scattering. The total contribution from all these processes to the observed π^0 and η peaks was evaluated as 3 events and <1 event respectively.

The contribution from beam-gas interactions was estimated by examining the shapes of the photon showers in the liquid argon, and projecting the direction of the showers back on to a plane passing through the beam line and parallel to the layers of the liquid argon module (The reconstruction program did not constrain the direction of the showers). In this way it was possible to estimate X, the point of origination of the showers. For each $\gamma\gamma$-pair, with the contribution from each photon weighted according to the size and shape of its shower, the position of X was calculated (a) perpendicular to the beam line (b) along the beam line. X is measured to an accuracy of typically ± 20 cm in each direction. Although the measurement of the position perpendicular to the beam line is sufficiently accurate to distinguish between reactions on the beam line and those occurring in the beampipe (at a radius of 10 cm), it does allow a small number of very anomalous events to be isolated which are completely incompatible with originating from the beam line. These were attributed to cosmics and removed from the events sample. The position of X along the beam line for the remaining events indicates a small number of events originating away from the interaction point, and attributable to beam-gas interactions. These were removed, and a correction of $2\pm 2\%$ applied to the remaining event sample to allow for the presence of further events of this type.

Table 1. Values for the $\pi^0-\gamma$-transition form factor and number of MC predicted events for ρ-pole dominance

Q^2 [GeV^2]	$\langle Q^2 \rangle$	Data events	ρ-MC events	$F^2(Q^2)m^3/64\pi$ [eV]
0.5–0.8	0.68	40.7 ± 6.6	42.8	1.56 ± 0.26
0.8–1.1	0.94	37.9 ± 6.4	39.8	1.07 ± 0.18
1.1–1.5	1.26	24.1 ± 5.1	30.6	0.59 ± 0.13
1.5–2.1	1.70	17.6 ± 4.4	16.8	0.52 ± 0.13
2.1–2.7	2.17	6.5 ± 2.6	3.9	0.59 ± 0.23

To investigate beam-gas interactions further, data were taken over a period of several days with the electron and positron beams laterally separated. These data corresponded to a few per cent of the luminosity of the data, which did not allow a quantitative background to be estimated, but it was possible to gain an understanding of some of the general features of the beam-gas events. The small numbers of tagged events were found to be dominated by low energy forward signals, none above 6 GeV. No event survived the analysis cuts.

The events were finally subjected to a full kinematic fit, constraining the photon pair to a π^0 or η mass as appropriate, to establish the Q^2 value of each event. Monte Carlo events were generated corresponding to roughly ten times the data luminosity in each case, incorporating photon form factors governed by ρ-pole dominance. These events were passed through a detector simulation, using the EGS shower generator to generate the lead liquid argon energy deposits. They were finally analysed in the same way as the data. π^0 and η peaks are obtained of similar widths and masses to those of the data. The η signal will be discussed in the next section.

In Table 1, the numbers of π^0 events in the data are compared with the numbers of Monte Carlo events for different Q^2 intervals. The Monte Carlo used the standard decay width of the π^0 into two photons [11], with a ρ pole form factor of mass 0.770 GeV at each vertex. Good agreement is observed. In the end cap, 0.7 events are predicted and 1 ± 2 observed. These figures correspond to a pion form factor $F^2(Q^2)$ as illustrated in Fig. 5.

The total number of forward tagged π^0's, corrected for background, is $137\pm 12\pm 16$, where a systematic error of 12% dominated by uncertainties in the photon simulation is estimated. This agrees well with the Monte Carlo prediction of 134 events using ρ-pole dominance.

One possible double-tagged π^0 was found, in our data, compared with 3 predicted from the Monte Carlo. While this does not amount to a significant discrepancy, it draws our attention to the fact that there is no reason for the form factor of the softer virtual photon to be the same as that for the harder. Indeed, isospin conservation actually forbids the $I=1$ π^0 from coupling to the virtual $I=1$ particles such as ρ's, and the most natural scheme to use comprises a virtual ρ and a virtual ω. Experimentally, a ρ and an ω pole are difficult to distin-

guish from two ρ poles. Our data are well-described by the simple two-ρ-pole formula used in Monte Carlo. Fits to the measured form factor yielding a more quantitative result are described in Sect. 7.

4 The η form factor

For the determination of the $\eta\gamma^*\gamma$-transition form factor the η decay channels $\pi^+\pi^-\pi^0$ and $\pi^+\pi^-\gamma$ were studied, in addition to the decay $\eta\to\gamma\gamma$.

Owing to the low Q-value of the hadronic decay modes, the photon detection probability is quite low, and these two decay modes are indistinguishable when only one photon is recorded in the detector. To select events solely stemming from the decay into $\pi^+\pi^-\pi^0$ two photons have to be detected.

For the selection of the 2 charged prong final states a maximum track momentum of 10 GeV and a minimum acoplanarity and acollinearity of 2° were demanded to reject annihilation events. To allow for photons in the final state the squared sum of transverse track momenta had to be larger than 0.005 GeV^2.

The invariant mass spectrum of the two photons in the corresponding data sample shows a clear π^0-peak. Events with the $\gamma\gamma$-mass in the π^0-band (70–190 MeV) are subjected to full kinematical fit with a π^0-mass constraint. The resulting invariant mass spectrum of the three pions shows a clean peak of 6 events at the η-position. These events are distributed over the Q^2-range covered by the forward spectrometer. No event with an end cap tag is observed.

Much higher statistics is achieved by only demanding one photon in the final state. These events are subjected to a kinematical fit requiring transverse momentum balance. Only events surviving this fit with a χ^2-probability of $>2\%$ and with a photon energy above 100 MeV are considered further. The number of η-candidates in the $\pi^+\pi^-\gamma$-spectrum is determined in the signal region (420–540 MeV) with the contribution from two sidebands (300–420 MeV and 540–600 MeV) subtracted. From the MC studies it was established that most of the decays observed stem from incompletely reconstructed $\pi^+\pi^-\pi^0$-events, the level of genuine $\pi^+\pi^-\gamma$-events being only of the order of 10%. To calculate the correct number of expected MC events in the signal region the two decay modes were generated according to the ratio of their corresponding branching ratios (4.91% $\pi^+\pi^-\gamma$ and 23.7% $\pi^+\pi^-\pi^0$). The number of data events in the tagged Q^2-range was compared to the number of generated events from these two sources to give the Q^2-development of the form factor.

The selection of the $\gamma\gamma$ decay mode has already been described in Sect. 3. After subtraction of the contributions from the sidebands, 40.6 ± 8.5 η-candidates remaining in this channel. From these the Q^2-development of the form factor was evaluated.

The form factors obtained from the $\eta\to\pi^+\pi^-\gamma(\gamma)$ and $\eta\to\gamma\gamma$ events were found to be in excellent agreement. The total number of η-candidates from all decay modes studied is 68.6 ± 11.1. Combined, they give the form factor values of Table 2 and Fig. 5. The $Q^2=0$ point ($\Gamma_{\gamma\gamma}=0.51$ keV) is taken from an average of the results of recent two-photon experiments which measured the radiative width of the η [11, 12].

Table 2. Combined values for the $\eta-\gamma$-transition form factor

Q^2 [GeV^2]	$\langle Q^2\rangle$	Data events	flat MC events	$F^2(Q^2)m^3/64\pi$ [eV]
0.3–0.8	0.62	21.8 ± 5.9	134	0.162 ± 0.044
0.8–1.2	1.02	21.3 ± 5.9	287	0.074 ± 0.028
1.2–1.7	1.43	12.6 ± 5.7	294	0.043 ± 0.020
1.7–3.4	2.23	12.9 ± 4.5	345	0.037 ± 0.013

5 The η'-radiative width

With the given experimental setup and trigger conditions the only pseudoscalar meson that can be observed in the CELLO detector in an *untagged* two-photon reaction is the η' in its decay mode $\rho\gamma$. This reaction has been studied to give a precise measurement of the coupling of the η'-meson to two almost real photons, i.e. at $Q^2\approx0$.

A data sample of about 20000 events with two charged tracks, one identified photon and no additional energy in the forward or end cap calorimeters above 1 GeV ("anti tag" condition) was searched for this resonance. The final-state particles of these untagged events should have balanced transverse momentum. This condition can be used to recalculate the photon energy, which is the least well measured particle parameter (all track parameters and the angles in the calorimeter are precisely measured). Multiplying the measured photon energy by a scale factor of $p_t(\pi\pi)/p_t(\gamma)\cdot|\cos\varphi(\pi\pi,\gamma)|$ minimizes the overall transverse momentum of the event and improves the resolution of the final state mass spectrum. From this spectrum the radiative width of the η' can be calculated if the spectrum is compared to the MC expectation for this reaction. This determination was performed in two ways: (1) counting the number of η'-candidates in the peak and (2) by fitting the mass spectrum with a polynomial background and the MC expected shapes for the η' and $a_2(1320)$ resonances.

To achieve a clean η' signal for method (1) a transverse momentum cut of $|\sum\mathbf{p}_t|^2<0.001$ GeV^2 was applied to the data. Events in the ρ-band (500–820 MeV) with a photon energy above 130 MeV were split into a signal region (0.92–1.00 GeV) and two sidebands (0.76–0.84 and 1.08–1.16 GeV). The number of η'-candidates determined from these regions is 668 ± 27 after background subtraction. With a branching ratio $B(\eta'\to\rho\gamma)$ of 30.1% [11] a radiative width of $3.62\pm0.14(\text{stat.})\pm0.48(\text{syst.})$ keV is obtained. The systematic error of 13% arises from the luminosity determination (3%), background subtraction (3%), trigger simulation (5%), a variation of the photon energy cut (4%), the track reconstruction (4%) and photon detection efficiency (8%), and the error on the branching ratio (5%).

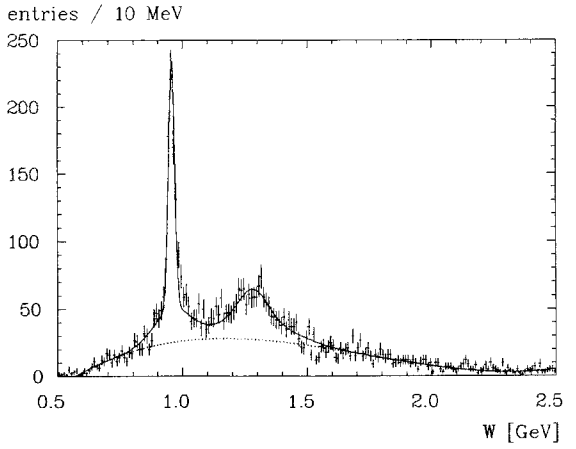

Fig. 2. Invariant $\pi^+\pi^-\gamma$-mass spectrum for untagged events with $p_t^2 < 0.01$ GeV^2. Shown are the results of a fit to the data spectrum using the MC predicted shapes

In method (2), the MC predicted shapes of the resonance and various parameterisations for the background were used to fit mass spectrum. To study systematic effects, different maximum transverse momentum cuts and minimum photon energy cuts were applied to the data. Figure 2 shows the mass spectrum obtained with a cut of $|\sum \mathbf{p}_t|^2 < 0.01$ GeV^2. The maximum deviation found by varying the cuts and background parametrisations is of the order of 5%. Complete agreement between the two methods is obtained:

$$\Gamma_{\gamma\gamma} \cdot \mathrm{B}(\eta' \to \rho\gamma) = 1.09 \pm 0.04(\mathrm{stat.}) \pm 0.13(\mathrm{syst.})\ \mathrm{keV}$$

$$\Gamma_{\gamma\gamma} = 3.62 \pm 0.14(\mathrm{stat.}) \pm 0.48(\mathrm{syst.})\ \mathrm{keV}.$$

The latter figure is in excellent agreement with the radiative widths found by other high statistics experiments in the $\rho\gamma$ and $\eta\pi^+\pi^-$ final states. Some experiments quote larger values for the radiative width, but their results are consistent with the above if the systematical errors are properly taken into account. A thorough discussion of the current situation based on published and new preliminary data for the radiative width of the η' can be found in [12].

6 The η' form factor

Qur determination of the η' form factor made use of the *tagged* decay modes $\eta' \to \rho\gamma$, $\eta' \to \pi^+\pi^-\eta \to \pi^+\pi^-\gamma\gamma$ and for the first time, $\eta' \to \pi^+\pi^-\eta \to \pi^+\pi^-\pi^+\pi^-(\pi^0/\gamma)$. The selection of the final states with two charged particles follows the same line as for the η. For the final state with four charged tracks events with exactly 2 positive and 2 negative charged tracks were selected. In addition a data sample with 2 and 3 charged tracks was prepared. A modified version of the reconstruction program optimised for low momentum tracks searched for additional tracks down to momenta of 50 MeV. We then kept all events from the two data samples with all tracks within $|\cos\vartheta| < 0.95$, ϑ being the polar angle of the track with respect to the beam axis. In addition we demanded that the tag be located opposite to the 4π-system in the $r\phi$-plane by a cut of $\varphi_{\mathrm{tag},4\pi} > 160°$.

A majority of events is found in the $\rho\gamma$-decay mode of the η', with the ρ decaying into two charged pions. A kinematical fit requiring $p_\perp$-balance is applied to all events with two oppositely charged pions and a single photon. The mass spectrum of events surviving this fit with a χ^2-probability of $>2\%$ shows a clear η'-signal. A cut in the photon energy of 50 MeV, a selection of events in the ρ-band (0.50–0.82 GeV) and a cut in the decay angle of the π in the ρ-helicity frame of $|\cos\vartheta_\pi^*| < 0.85$ leaves most of the signal and considerably reduces the level of background. The number of η'-candidates was determined from this spectrum by subtracting a hand drawn background. The total number of events obtained is 41.0 ± 7.7. These events are now split into 5 bins of Q^2, four covering the acceptance region of the forward calorimeter and one covering the end cap calorimeter. The number of events found in each bin is compared to the MC expectation for the reaction assuming a flat form factor dependence. The systematic error for these data points is 23%, with contributions from the luminosity determination (3%), photon detection (8%) and track reconstruction (4%) efficiencies, trigger simulation (6%), background subtraction (15%) and a variation of the photon energy cut (10%).

For the full reconstruction of the decay mode $\eta' \to \eta\pi^+\pi^-$, $\eta \to \gamma\gamma$ both photons have to be observed in the detector. The invariant $\gamma\gamma$-mass shows a clear π^0-signal; however, the expected small η-signal is submerged in a larger background of photon combinations from higher multiplicity states. Events in the η-band (310–720 MeV, taken from MC) were subjected to a full kinematical fit with an η-mass constraint for the two photons. The resulting invariant $\eta\pi^-\pi^-$-mass spectrum shows a background-free η'-signal of 10 events. The observed data events and the generated MC events are divided into the Q^2-bins, to be combined later with the data from the other channels.

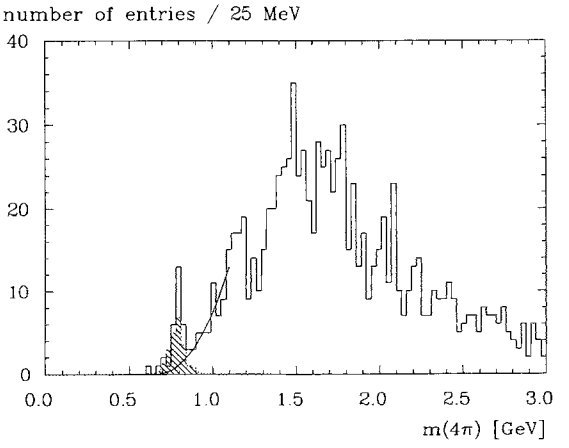

Fig. 3. Invariant 4π-mass spectrum. The shaded histogram marks the MC prediction for the reaction $\eta' \to \eta\pi^+\pi^-$ with $\eta \to \pi^+\pi^-(\pi^0/\gamma)$ using a ρ pole form factor

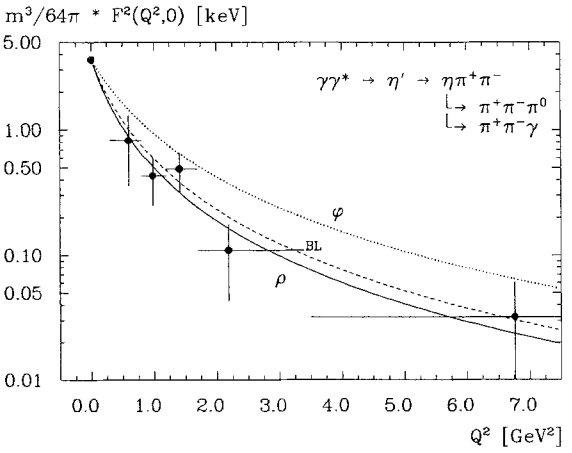

Fig. 4. Q^2-evalution of the $\eta' - \gamma$ transition form factor in the reaction $\eta' \to \eta\pi^+\pi^-$ with $\eta \to \pi^+\pi^-(\pi^0/\gamma)$. Shown are also the predictions for a ρ and ϕ-VDM form factor and the QCD-prediction by Brodsky and Lepage

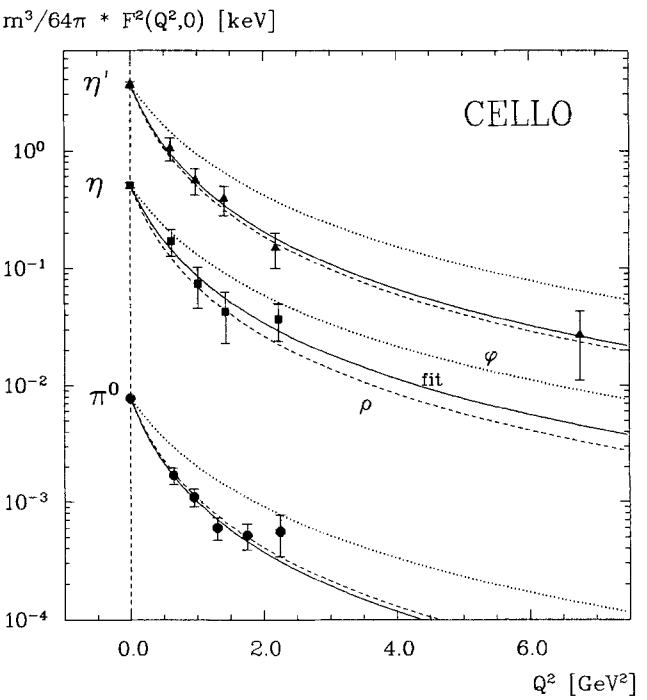

Fig. 5. Measured form factors for π^0, η and η', compared with ρ and ϕ-pole dominance. The solid lines mark the result of a fit to the data points. The $Q^2=0$ points for the π^0 (life time) and η (average of two-photon experiments) are taken from [11, 12]

The $\eta\pi^+\pi^-$-decay mode of the η'-meson has for the first time been observed in a tagged two photon reaction in the η-decay modes into $\pi^-\pi^-\gamma$ and $\pi^-\pi^-\pi^0$. Owing to the low Q-value of this reaction the final state can safely be identified without the detection of the photons. In fact, the contribution of the photons to the total transverse momentum of the events is so small that even without their measurement a kinematical fit requiring transverse momentum balance can be used to improve the Q^2-resolution of the tagged virtual photon. The resulting 4π-invariant mass spectrum is shown in Fig. 3 showing a clear signal from the η' decay together with the MC prediction for this reaction using a ρ-pole form factor. The full line in the plot is the hand drawn background subtracted from the spectrum, yielding 25.0 ± 5.6 η'-candidates. The resulting values for the quantity $m^3/64\pi \cdot F^2(Q^2, 0)$ are shown in Fig. 4. For $Q^2=0$ this quantity is equal to the radiative width of the resonance. The main systematic uncertainties for this decay mode stems from the variation of the polar angular cut between $|\cos\vartheta|<0.88$ and $|\cos\vartheta|<0.95$ and a variation of the background shape. Comparable results are obtained if no kinematical fit is applied. The resulting systematic error is of the order of 30% with negligible contributions from trigger simulation, luminosity determination and track reconstruction efficiency.

Table 3. Combined values for the $\eta' - \gamma$-transition form factor. These numbers combine the results from the η'-decays into $\rho\gamma$ and $\eta\pi^+\pi^-$, with a subsequent decay of the η into $\gamma\gamma$, $\pi^+\pi^-\gamma$ and $\pi^+\pi^-\pi^0$

Q^2 [GeV²]	$\langle Q^2 \rangle$	Data events	Flat MC events	$F^2(Q^2)m^3/64\pi$ [keV]
0.3– 0.8	0.62	26.0 ± 5.9	24.7	1.05 ± 0.24
0.8– 1.2	1.02	20.0 ± 5.1	35.7	0.56 ± 0.14
1.2– 1.7	1.43	15.0 ± 4.4	38.5	0.39 ± 0.11
1.7– 3.4	2.23	10.5 ± 3.6	71.7	0.15 ± 0.05
3.4–20	7.0	4.5 ± 2.6	167.9	0.027 ± 0.016

Since all three decay channels have been evaluated independently, a combination improves the statistical significance and greatly reduces the influence of the various sources of systematic errors. The total number of η'-candidates from all sources is 76 ± 10. The Q^2-development of the transition form factor derived from these events is given in Table 3 and Fig. 5. The four Q^2-points in the range of the forward calorimeter and the one end cap calorimeter point are complemented by our measurement of the radiative width of the η'-meson at $Q^2=0$ (Sect. 5).

7 Fits to the form factors

All the measured pseudoscalar form factors show the expected strongly falling behaviour for increasing values of Q^2, which is well described by a simple ρ-pole. To arrive at a more quantitative result a pole fit with $F(Q^2)=A/(1+Q^2/\Lambda_P^2)$ has been performed on all measured form factors, with Λ_P being the pole mass for a given pseudoscalar meson P. These Λ_P do not necessarily have to be the same. Quantitative predictions exist in the frame work of VDM exploiting the known quark contents of the pseudoscalar mesons. Here, the Λ_P are combinations of the vector meson masses m_ρ, m_ω and m_ϕ, with the major contribution from the ρ-meson. The pole masses are predicted to be [7] $\Lambda_{\pi^0}=0.77$ GeV, $\Lambda_\eta=0.73$ GeV and $\Lambda_{\eta'}=0.82$ GeV. In a QCD inspired interpolation formula by Brodsky and Lepage [13], the pole mass Λ_P is identified with the quantity $2\pi\sqrt{2}\,f_P$, where f_P is the PCAC coupling constant of the pseudoscalar meson. The interpolation in [13] is performed for

Table 4. Results of pole-fits to the form factors

P	Λ_P [MeV]	f_P [MeV]	b_P [GeV^{-2}]	a_P	r_P [fm]
π^0	748 ± 30	84 ± 3	1.79 ± 0.14	0.0326 ± 0.0026	0.65 ± 0.03
η	839 ± 63	94 ± 7	1.42 ± 0.21	$0.428\ \pm0.063$	0.58 ± 0.04
η'	794 ± 44	89 ± 5	1.59 ± 0.18	$1.46\ \ \pm0.16$	0.61 ± 0.03

the π^0 between (i) $Q^2=0$ limit for $F(Q^2)$, which is given by the experimental rate for the decay $P\to\gamma\gamma$ and implied by current algebra to be proportional to $1/f_\pi^2$, and the (ii) $Q^2\to\infty$ limit $F(Q^2)\propto f_\pi/Q^2$. The same high Q^2 limit for the π^0 and η was also derived by Walsh and Zerwas [15]. With the measured pion decay constant f_π of 93 MeV [14] a pole mass of $\Lambda_{\pi^0}=0.827$ GeV is predicted. If all pseudoscalar decay constants are identical then so are the pole masses for the corresponding form factors. For charged pions Chung et al. [10] have shown that the quark model is capable of giving rise to form factors equivalent to ρ-pole dominance.

Alternatively, one can expand the form factor around $Q^2=0$ into a linear form of the type $A\cdot(1-b_P\cdot Q^2)$ [7] or $A\cdot(1-a_P\cdot Q^2/m_P^2)$ [11], which is the usual parametrisation in conversion ("Dalitz pair") decay experiments. The quantities a and b can easily be related to the pole masses in the above ansatz. The slope b of the form factor at $Q^2=0$ is related to the size r of the interaction region at the $P-\gamma\gamma^*$-vertex by $r=\sqrt{6\cdot b}$.

The results of the pole form fit to the pseudoscalar$-\gamma\gamma^*$-transition form factor are shown in Table 4. In these fits only the statistical errors of data points have been taken into account. It is of interest to compare the results with measurements obtained from different two-photon experiments and from conversion decay experiments. For the η' a pole mass fit has been performed by the TPC/2γ Collaboration [16] in the Brodsky-Lepage parametrisation yielding $f_{\eta'}=96\pm8$ MeV. The PLUTO [17] and Mark II [18] collaborations measured also the η' form factor but performed no pole fit on the data points. Their results are however in qualitative agreement with our findings. The Lepton-G Collaboration [19] has measured the slope of the form factor in the reaction $\eta'\to\mu^+\mu^-\gamma$ to be $b=1.7\pm0.4$ GeV^{-2}. These results correspond to pole masses of 0.85 ± 0.07 GeV (TPC/2γ) and 0.77 ± 0.18 GeV (Lepton-G), both in good agreement with our value of 0.79 ± 0.04 GeV. Averaging the three results leads to a pole mass of $\Lambda_{\eta'}=0.81\pm0.04$ GeV.

For the η, only one other measurement of the form factor in the space-like region exists. The TPC/2γ Collaboration [16] measured $f_\eta=122\pm13$ MeV (corresponding to a pole mass of 0.70 ± 0.08 GeV). In the time-like region the Lepton-G Collaboration [20] used the reaction $\eta\to\mu^+\mu^-\gamma$ to determine the slope b of the form factor at $Q^2=0$. They find $b_\eta=1.9\pm0.4$ GeV^{-2} ($\Lambda_\eta=0.72\pm0.09$ GeV). Our result of $\Lambda_\eta=0.84\pm0.06$ GeV is compatible with these two results within errors. The combined result of 0.77 ± 0.04 GeV is equivalent to the mass of a ρ-pole.

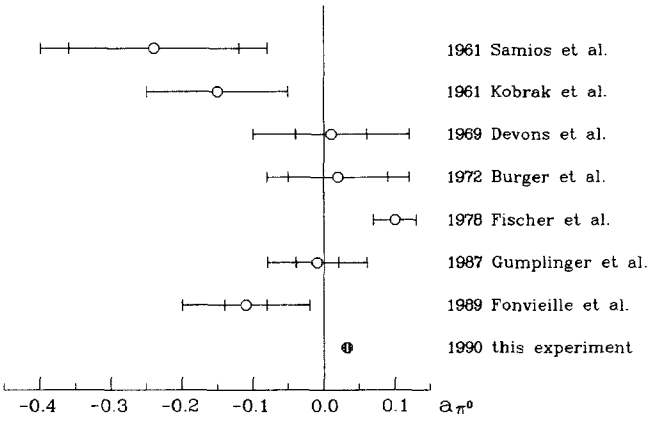

Fig. 6. Values of the form factor slope parameter a. The inner error bars denote the statistical errors, the outer ones the total error. Data have been taken from [11]

Our measurement of the π^0-form factor in the space-like region solves a long standing problem. The measurements of the slope of the form factor in the time-like region can only be performed in the reaction $\pi^0\to e^+e^-\gamma$. Due to the small kinematic region, the background situation and the need for final-state radiative corrections, large systematical uncertainties govern the slope measurement of the form factor, and even high statistics experiments have not been able to agree on the sign for the slope a_{π^0}. Figure 6 shows the current situation. The published values for a range from -0.24 to $+0.10$. Note that some of the experiments have only given statistical errors. The systematical error of our determination of a_{π^0} is of same order as the statistical error quoted in the Table 4. Our value of $a_{\pi^0}=0.0326\pm0.0026$ (corresponding to $\Lambda_{\pi^0}=0.75\pm0.03$ GeV) is well in accord with the predictions for this quantity from VDM and QCD calculations. Measurements of the charged pion radius in the space-like region yield results which are in exact agreement with our measured size $r=0.65\pm0.03$ fm of the $\pi^0-\gamma\gamma$-vertex. Amendolia et al. [6] found a charged pion radius of $r=0.657\pm0.012$ fm in πe-scattering data using a pole form for the fit. Similar results for charged pions are reported in this reference from other experiments in the time-like and space-like region.

8 Summary and conclusions

We have measured the pseudoscalar-γ transition form factors for the π^0, η and η' in a variety of decay modes. A fit to the data points for each of the measured form factors using a pole form yields quantitative results which are in good agreement with results obtained by other experiments in two-photon reactions, leptonic conversion decays and scattering experiments, covering the space-like and time-like region. Our measurement of the neutral pion form factor, which is well in accord with the corresponding measurement for charged pions, re-

solves a long standing confusion about the sign of the neutral pion form factor slope. All measured form factors are well described by a pole form. The fit parameters are interpreted in three completely different ansatzes: in the VDM picture, QCD inspired calculations and finite size models. Since it is not obvious that all these descriptions are equivalent, it is interesting to note that our measurements give results in the expected range: the ρ-mass in VDM, the pseudoscalar decay constant f_π in QCD and an effective size of the interaction region which is equal to the charged pion radius.

Acknowledgements. We gratefully acknowledge the outstanding efforts of the PETRA machine group which made possible these measurements. We are indebted to the DESY computer centre for their excellent support during the experiment. We acknowledge the invaluable effort of the many engineers and technicians from the collaborating institutions in the construction and maintenance of the apparatus. The visiting groups wish to thank the DESY Directorate for the support and kind hospitality extended to them. This work was partly supported by the Bundesministerium für Forschung und Technologie (Germany), by the Commissariat à l'Energie Atomique and the Institut National de Physique Nucléaire et de Physique des Particules (France), but the Istituto Nazionale di Fisica Nucleare (Italy), by the Science and Engineering Research Council (UK) and by the Ministry of Science and Development (Israel).

References

1. C.J. Bebek et al.: Phys. Rev. D16 (1977) 1986; C.J. Bebek et al.: Phys. Rev. D17 (1978) 1693
2. G. Bardin et al.: Nucl. Phys. B120 (1977) 45
3. S.F. Berezhnev et al.: Sov. J. Nucl. Phys. 16 (1973) 99
4. G.T. Adylov et al.: Phys. Lett. 51B (1974) 402; S. Dubnicka, O.V. Dumbrajs: Phys. Lett. 53B (1974) 285
5. E.B. Dally et al.: Phys. Rev. Lett. 39 (1977) 1176
6. S.R. Amendolia et al.: Phys. Lett. 146B (1984) 116
7. L.G. Landsberg: Phys. Rep. 128 (1985) 301
8. H.-J. Behrend: Comp. Phys. Comm. 22 (1981) 365
9. H.-J. Behrend et al.: Phys. Scr. 23 (1981) 610
10. P.L. Chung, F. Coester, W.N. Polyzou: Phys. Lett. B205 (1988) 545
11. Particle Data Group: Review of Particle Properties. Phys. Lett. B204 (1988)
12. J.H. Peters: Ph.D. Thesis, Univ. Hamburg, 1990, Internal Report DESY FCE-90-01
13. S.J. Brodsky, G.P. Lepage: Phys. Rev. D24 (1981) 1808
14. In [11] $f_P = 131.69$ MeV is quoted in a notation that is a factor $\sqrt{2}$ larger than that used in this paper
15. T.F. Walsh, P. Zerwas: Nucl. Phys. B41 (1972) 551
16. TPC/2γ Coll. H. Aihara et al.: Phys. Rev. Lett 64 (1990) 172
17. PLUTO Coll. Ch. Berger et al.: Phys. Lett. 142B (1984) 125
18. Mark II Coll. G. Gidal et al.: Phys. Rev. Lett. 59 (1987) 2012
19. Lepton-G Coll. R.I. Dzhelyadin et al.: Phys. Lett. 88B (1979) 379
20. Lepton-G Coll. R.I. Dzhelyadin et al.: Phys. Lett. 94B (1980) 548